Journal of Non-Crystalline Solids xxx (2016) xxx–xxx

Contents lists available at ScienceDirect

Journal of Non-Crystalline Solids

journal homepage: www.elsevier.com/locate/jnoncrysol

Effect of Ce addition on the glass-forming ability and hard-magnetic properties of the Nd-Fe-Al bulk metallic glasses

Y.C. Lu, Q. Bai *, L. Bian, H. Xu, S. Xia

Laboratory for Microstructures, Shanghai University, Shanghai 200444, China

ARTICLE INFO

Article history:
Received 24 August 2016
Received in revised form 14 October 2016
Accepted 16 October 2016
Available online xxxx

Keywords:
Suction casting
Glass-forming ability
Hard magnetic behavior

ABSTRACT

The influence of Ce addition on the glass-forming ability (GFA) and hard-magnetic properties of the $Nd_{60-x}Ce_xFe_{30}Al_{10}$ ($x = 0-35$) alloy prepared by suction casting have been investigated. The glass-forming ability of the as-cast rods increased with the addition of Ce content from $x = 0$ to $x = 30$, and then decreased for $x = 35$. The as-cast rods with a composition of $x = 0$ and $x = 30$ contained two amorphous magnetic phases including Fe-rich regions and Nd-rich regions characterized by the Curie temperature T_{c1} and T_{c2}. The Ce atoms may be unevenly distributed in the two magnetic phases, which prefer to substitute Nd in the low T_c phase. All the alloys exhibit hard magnetic behavior, while the room-temperature coercivity and remanence gradually decrease with the Ce addition. The saturation magnetization (M_s), remanence (M_r) and coercivity ($_iH_c$) of the alloy for $x = 30$ with the best glass-forming ability are 16.30 Am^2/kg, 10.22 Am^2/kg and 162.31 kA/m, respectively.

1. Introduction

Since 1996, Nd-Fe-Al bulk amorphous alloys with large glass-forming ability (GFA) and hard magnetic behavior at room temperature were reported by Inoue et al. and other researchers [1–5]. From then on, more and more attentions have been paid to Nd-based amorphous alloys with hard-magnetic properties. Impelled by their potential applications such as the proper use in the cosmetic and dermatological field [6], recording disks [7,8], solenoid actuator [9] and permanent magnet motors in the modern cars [10] as well as fundamental research interests, much work [11–15] has been conducted to find new alloys with excellent glass-forming ability and good hard-magnetic properties. A number of rare earth-transition metal (RE-TM) based BMGs were prepared in a size of millimeters by copper mold casting. The amorphous $Pr_{60}Fe_{30}Al_{10}$ bulk alloy with 3 mm diameter was found to exhibit hard-magnetic properties of 0.089 T for B_r and 300 kA/m for $_iH_c$ by Inoue et al. [11]. Kong et al. [12] reported that the cast rod of $Sm_{60}Fe_{30}Al_{10}$ alloy with 1 mm diameter exhibited much lower coercivity than that of $Nd_{60}Fe_{30}Al_{10}$ alloy. The GFA [13] and the room temperature coercivity [14] for $Nd_{60-x}Y_xFe_{30}Al_{10}$ alloys were found to decrease with the increase of Y, but the $Nd_{60}Fe_{20}Al_{10}Y_{10}$ alloy exhibited the large GFA and could be cast into bulk amorphous cylindrical specimens of 3 mm in diameter. The coercivity of $Nd_{60-x}Fe_{30}Al_{10}Dy_x$ alloys increases markedly with increasing Dy content [15].

The preparation of the Nd-based alloys has attracted much attention due to their high GFA and hard magnetic behavior at room temperature. However, the high cost of Nd metal becomes the maximum limitation for their applications [16]. It is well known that Ce is the most abundant and low cost rare-earth element in the world. More recently, Ce has been introduced to the Al-based and La-based alloys. For example, Song et al. [17] found that Ce element can enhance the GFA and thermal stability of the Al-Ni-Si alloys. Zhang et al. [18,19] found that the partial substitutions of La by Ce can enhance the GFA of $Al_{86}Ni_9La_5$. Li et al. [20] reported that the coexistence of La and Ce with similar atomic size and various valence electronic structure obviously improves the GFA of $(La_xCe_{1-x})_{65}Al_{10}Co_{25}$ BMGs compared with the GFA of single-lanthanide-based alloys, $La_{65}Al_{10}Co_{25}$ and $Ce_{65}Al_{10}Co_{25}$. In our experiments, Ce was considered individually to be added into the $Nd_{60}Fe_{30}Al_{10}$ alloy showing hard magnetic behavior at room temperature. The properties of Nd-Ce-Fe-Al, including GFA, magnetic properties and microstructure mechanism were systematically assessed in this work.

2. Experimental

Alloy ingots with a nominal composition of $Nd_{60-x}Ce_xFe_{30}Al_{10}$ ($x = 0-35$) were prepared by arc-melting Nd, Ce, Fe, and Al with a purity of 99.9% (Beijing Huaxia Huiying Technology Development Co., Ltd) in a titanium-gettered argon atmosphere. The ingots were remelted several times to ensure homogeneity. Bulk cylindrical samples of 3-mm diameter and 50-mm length were prepared by copper mold suction casting. The samples in the form of ribbons were produced by melt-spinning at a copper roll having surface speed of 30 m/s. The structure of the samples was characterized by X-ray diffraction (Cu Kα). Thermal stability was examined by differential scanning calorimetry (DSC). Magnetic

* Corresponding author.
E-mail address: baiqin31@shu.edu.cn (Q. Bai).

http://dx.doi.org/10.1016/j.jnoncrysol.2016.10.024
0022-3093/

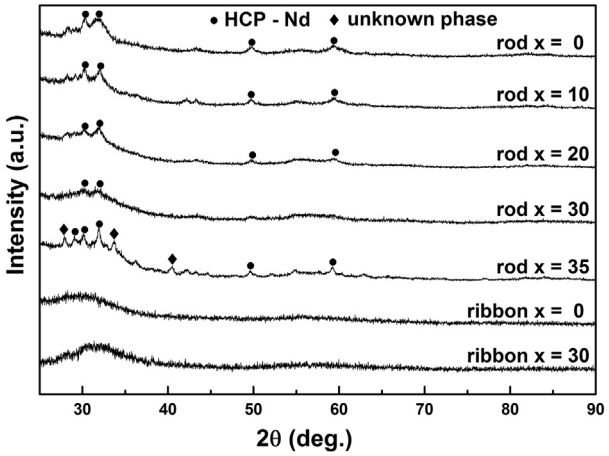

Fig. 1. XRD patterns for the as-cast $Nd_{60-x}Ce_xFe_{30}Al_{10}$ ($x = 0-35$) and as-spun $Nd_{60-x}Ce_xFe_{30}Al_{10}$ ($x = 0$ and 30) alloys.

hysteresis loops at room temperature were performed using a Lake Shore 7407 vibrating sample magnetometer (VSM) with a maximum magnetic field of 1.8 T. Thermomagnetic curves were measured by using a Quantum Design Physical Property Measurement System (PPMS) equipped with a 1 T magnet in the range 10 K to 650 K. The microstructure of samples was studied by a scanning electron microscope (SEM, JSM-6700F) equipped with an in-situ energy dispersive spectrometer (EDS) and transmission electron microscope (TEM, JEM 2010F) with a field emission electron gun operating at 200 kV.

3. Results and discussion

XRD patterns for the as-cast and as-spun $Nd_{60-x}Ce_xFe_{30}Al_{10}$ samples with various Ce doping are shown in Fig. 1. Some diffraction peaks over the large broad amorphous diffraction in the as-cast Ce-free alloy suggest that the sample is comprised of hexagonal Nd and partial amorphous phase. One bump is found in both ribbons at about 32° which revealed that the ribbons are fully amorphous. The volume fraction of the amorphous phase increases with the increasing Ce content from $x = 0$ to $x = 30$ for the as-cast rods. The as-cast samples nearly possess an entire amorphous diffraction peak when x reaches 30. This indicates that the proper content of Ce can improve the glass-forming ability of $Nd_{60-x}Ce_xFe_{30}Al_{10}$ alloys. The volume fraction of amorphous phase also decreased with the progressive Ce substitution in the sample for $x = 35$.

Table 1
Crystallization temperature T_x, Curie temperatures T_{c1}, T_{c2}, remanence M_r, intrinsic coercivity $_iH_c$, and saturation magnetization M_s for as-cast $Nd_{60-x}Ce_xFe_{30}Al_{10}$ ($x = 0-35$) alloys.

Alloys	T_x (K)	T_{c1} (K)	T_{c2} (K)	M_r (Am^2/kg)	$_iH_c$ (kA/m)	M_s (Am^2/kg)
$x = 0$	776.2	52.6	521.0	14.98 ± 0.02	287.51 ± 0.5	22.13 ± 0.01
$x = 10$	784.9			13.02 ± 0.02	264.56 ± 0.5	19.35 ± 0.01
$x = 20$	754.9			10.60 ± 0.02	203.74 ± 0.5	17.14 ± 0.01
$x = 30$	716.6	30.3	476.7	10.22 ± 0.02	162.31 ± 0.5	16.30 ± 0.01
$x = 35$	650.3			6.39 ± 0.02	120.77 ± 0.5	13.36 ± 0.01

In order to further understand the glass-forming ability of the as-cast cylinders, the as-cast and as-spun samples were examined by DSC. Fig. 2 shows typical DSC curves for the as-cast $Nd_{60-x}Ce_xFe_{30}Al_{10}$ ($x = 0-35$) and as-spun $Nd_{60-x}Ce_xFe_{30}Al_{10}$ ($x = 0$ and 30) alloys at a constant heating rate of 0.33 K/s. The exothermic signals can be attributed to the crystallization indicating that these specimens contain amorphous phase. It can be seen that neither glass transition nor super cooled liquid region before crystallization is observed. These phenomena are consistent with the previously published results on Nd-based amorphous alloys [1,2,4,5,13,14]. The absence of glass transition temperature and supercooled liquid region in these alloys was explained by Sun et al. [21] as the result of continuous growth of the Nd nanocrystalline phase. Another explanation was that the continuous occurrence of glass transition in a large temperature scale according to Wei et al. [22]. As marked with the arrows in Fig. 2, the melting temperature (T_m) decreases with the increasing Ce content due to the low melting point of Ce element. The increasing of onset crystallization temperatures (T_x) from $x = 0$ to $x = 10$ indicates that the thermal stability of the as-cast alloys increase with small Ce substitution. But with the progressive Ce substitution, the onset crystallization temperature (T_x) decreases from $x = 20$ to $x = 35$ which indicates that the thermal stability decreases. All the values of T_x are listed in Table 1. The ratio of exothermic enthalpy to endothermic enthalpy for the as-cast $Nd_{60-x}Ce_xFe_{30}Al_{10}$ ($x = 0-35$) alloys were determined to be 0.4206, 0.4646, 0.4860, 0.5968 and 0.2991, respectively, which properly means the $x = 30$ composition has the most amorphous phase. In order to further analyze the glass-forming ability of the as-cast alloys. The ribbons of $Nd_{60-x}Ce_xFe_{30}Al_{10}$ ($x = 0$ and 30) were examined by DSC. The XRD patterns revealed that the ribbons were fully amorphous. The ratios of exothermic enthalpy to endothermic enthalpy were calculated to be 0.4916 and 0.6090 for the ribbons, while 0.4206 and 0.5968 for the rods. Because the ribbons were fully amorphous, the volume fraction of amorphous phase in the as-cast $Nd_{60-x}Ce_xFe_{30}Al_{10}$ ($x = 0$ and 30) samples were 0.4206 / 0.4916 = 85.56% and 0.5968 / 0.6090 = 97.99%. So the volume fraction of amorphous phase increased

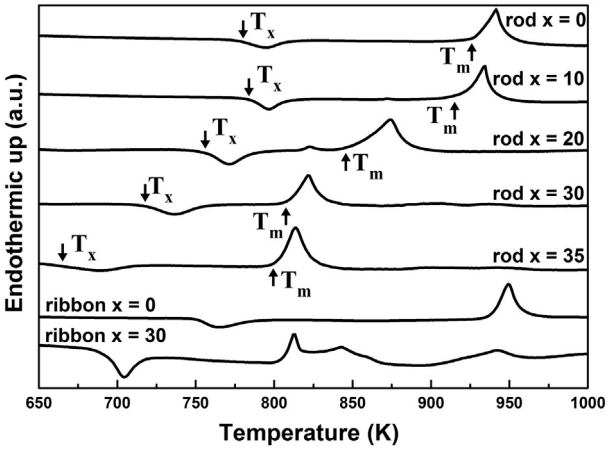

Fig. 2. DSC curves for the as-cast $Nd_{60-x}Ce_xFe_{30}Al_{10}$ ($x = 0-35$) and as-spun $Nd_{60-x}Ce_xFe_{30}Al_{10}$ ($x = 0$ and 30) alloys.

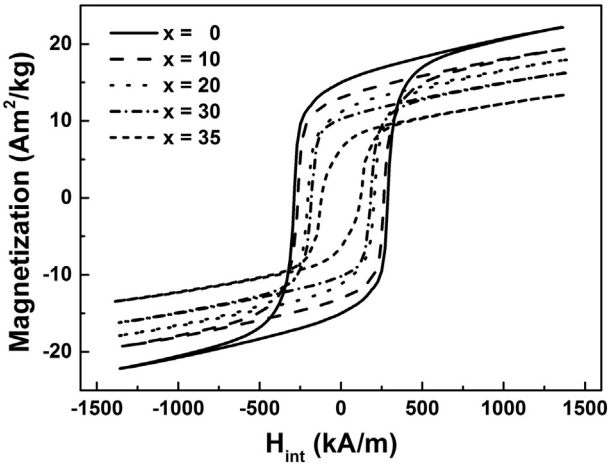

Fig. 3. Hysteresis loops for the as-cast $Nd_{60-x}Ce_xFe_{30}Al_{10}$ ($x = 0-35$) alloys.

Please cite this article as: Y.C. Lu, et al., Effect of Ce addition on the glass-forming ability and hard-magnetic properties of the Nd-Fe-Al bulk metallic glasses, J. Non-Cryst. Solids (2016), http://dx.doi.org/10.1016/j.jnoncrysol.2016.10.024